PAPER

Check for updates

Synthesis of gypsum fertilizer from waste eggshells for a sustainable environment

Md. Sahadat Hossain, [ID] [a] Md. Aftab Ali Shaikh[ac] and Samina Ahmed [ID] *[ab]

In this research, waste eggshells were used as the source of calcium to synthesize valuable gypsum fertilizer. Three different routes were used to synthesis gypsum, namely (i) direct synthesis from raw eggshells; (ii) synthesis from calcium oxide as obtained after calcination of eggshell; and (iii) synthesis after production of calcium hydroxide from calcium oxide. Several batches from the three routes produced very similar results and the products were characterized by X-ray diffraction, Fourier-transform infrared spectroscopy, scanning electron microscopy, and thermogravimetric and energy dispersive X-ray (EDX) analyses. A set of test procedures such as free water calculation, combined water measurement, pH, and conductivity estimation were performed in addition to the highly sophisticated characterization techniques. A few properties of gypsum were compared in aqueous medium and soil extraction. Different crystallographic parameters such as lattice parameters, crystallite size, dislocation density, microstrain, and growth preference were computed from the XRD data.

Introduction

Environment friendly production and consumption for sustainable development have been rated as the top priority issues in recent years.[1] The gradual depletion of the environment is intensifying the need to minimize or reduce pollution levels. The word sustainability is related to the future of humanity, the reliability of resources and ecology for the continued existence of mankind as it connects social elements, the economy, and environmental issues.[2] In various countries, there is a scarcity of food, even though one-third of the total produced food is cast-off as waste or lost in different ways. This waste or loss not only causes a shortage of food but also adversely affects the environment by wasting land, water and fertilizer which are consumed for food production.[3] The utilization of waste food or discarded parts of food can be an inevitable part of the approach to a sustainable environment. Waste eggshells are one of the most discarded food parts and are mainly composed of $CaCO_3$, a natural source of calcium. Nearly 76.7 million tons of eggs were produced in 2018 around the world[4] and the quantity is increasing day by day. About 10% of total egg composition/mass is eggshell and the calcium carbonate content in eggshell varies from 95 to 97% which can be a rich

source of calcium.[5] The synthesis of chemicals from natural resources or renewable sources is the driving force for environmental sustainability.[6] However, throwing out eggshells is economically and environmentally challenging. Being enriched with calcium, eggshells have extensive applications in various fields of materials science including biomedical applications and environmental engineering. Biomedical applications include soluble proteins, organic calcium, activated calcium, health-promoting products, food processing and production, *etc.*,[7] and industrial applications include reaction templates, reactors, catalysts, *etc.*[8,9] The utilization of eggshells as catalysts is increasing day by day in organic synthesis, turning waste oils into biodiesel, various industrial applications, catalyst modification, *etc.*[10–12] Investigations of the application of eggshells in synthesizing hydroxyapatite, tricalcium phosphate, and various bone like substances have been carried out in many previous studies.[13,14] Additionally, syntheses of other industrially important materials such as monocalcium/dicalcium/tricalcium phosphates have also been reported.[15] The use of eggshells in calcium sulphate form is another method of waste utilization. A few researchers have reported gypsum as a dietary supplement that provides calcium as well as sulphate.[16]

The demand for fertilizer is greatly influenced by the demand for food and the global population.[17] As the population of the world is drastically increasing, the need for food as well as fertilizers is also increasing in the same manner. Although nitrogenous nutrients are in prime demand, calcium and sulfate-based fertilizers are also essential for smooth plant growth. In the fertilizer sector, gypsum ($CaSO_4 \cdot 2H_2O$) is widely used as a source of Ca and SO_4^{2-} to minimize crusting, lessen

[a] Institute of Glass & Ceramic Research and Testing, Bangladesh Council of
  Scientific and Industrial Research (BCSIR), Dhaka-1205, Bangladesh.
  E-mail: shanta_samina@yahoo.com
[b] BCSIR Laboratories Dhaka, Bangladesh Council of Scientific and Industrial
  Research (BCSIR), Dhaka-1205, Bangladesh
[c] Department of Chemistry, University of Dhaka, Dhaka-1000, Bangladesh

erosion, and reduce phytotoxicity, to treat sodium enriched soil. A report from Ohio State University mentioned that gypsum is one of the oldest (more than 250 years) forms of nutrients applied to enhance soil fertility in the United States. Gypsum is also known as hydrous calcium sulphate due to the two moles of water in its crystal structure and is 150 times more soluble in water than calcium carbonate.[18] Gypsum is mainly found in natural deposits, as a by-product of manufacturing processes, in recycled waste wallboard, as a product of flue gas desulfurization, *etc.* and there are various patents registered in the US for gypsum synthesis[19] but none of them reported a synthesis process from bio-waste sources such as eggshells. However, anhydrite from duck eggshells was reported in the literature[20] where no in-depth analysis was reported from a crystallographic viewpoint.

In this research, the prime focus was concentrated on utilizing bio-waste (eggshell) to synthesize valuable products for environmental sustainability. Waste eggshells were picked as the source of calcium to produce gypsum fertilizer. Another aim of this research was to assist small entrepreneurs in setting up a small fertilizer industry for a sustainable approach.
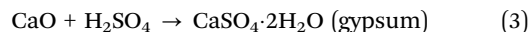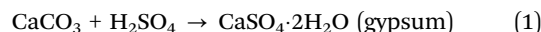
Materials and methods

Materials

Eggshells were collected from raw eggs and then cleaned with sufficient tap water followed by careful removal of the inner membrane. Simple air drying facilitated their further utilization to synthesize gypsum. However, prior to use, the eggshells were subjected to wavelength-dispersive X-ray fluorescence (WDXRF) analysis to determine their chemical composition. A preset operating mode (tube current 100 mA coupled with 50 kV) of WDXRF (ZSX Primus IV, Rigaku) enabled acquisition of the chemical composition (in oxide form) as: CaO (97.0%, maximum), MgO ($\sim$1.08%), Na_2O ($\sim$0.17%), P_2O_5 ($\sim$0.457%) along with different types of metal oxide.

Deionized water (DI) used throughout the study was prepared in the laboratory. The soil used to monitor the pH was collected from the periphery of the research laboratory. H_2SO_4 (concentration 98%) was purchased from Kuri Chemicals and no purification process was employed for further use.

Methods

Synthesis of gypsum. All the processed eggshells were finely ground using a ball mill (model: Pulverisette 5 classic line Planetary Ball Mill, speed: 400 rpm, time: 4 h, ball and lining material: zirconium oxide, condition: dry, size of balls: four different sizes, eggshell to ball ratio: 1 : 10) and mixed thoroughly for proper sampling. This powdered eggshell was directly used as the calcium source and stoichiometrically reacted with concentrated H_2SO_4 (concentration 98%) which resulted in a yield of 92 $\pm$ 3% according to eqn (1). The eggshell powder was calcined at 900 °C for 1/2 h to produce CaO by releasing CO_2 (eqn (2)). This CaO was used to synthesize the 2nd batch of gypsum according to the reaction as illustrated in

eqn (3). However, this 2nd route provided 89 $\pm$ 4% yield of gypsum, and the slightly lower yield may be due to the insignificant conversion of CaO to $Ca(OH)_2$ in an open environment which reduced the availability of calcium in reaction media. The 3rd pathway to synthesize gypsum was a combination of eqn (4) and (5) where CaO first reacted with water to form $Ca(OH)_2$ which subsequently reacted with H_2SO_4 (concentrated) to produce gypsum. In all the gypsum synthesis procedures the reaction medium was water. However, the final product was separated by the following two distinct ways: (i) the direct filtration of the solution; and (ii) by evaporation of water at 100 °C. When the filtration procedure was employed, the yield percentages were lower due to the solubility of gypsum. But, in the evaporation process, no such product loss occurred and a higher percentage of the product was obtained. No extra chemicals were engaged to maintain the pH of the solution as the aim was to develop a sustainable process by minimizing unnecessary chemicals, whether the additional chemicals are environmentally toxic or not. Several batches from the mentioned three processes were tested, with similar results recorded.

$$CaCO_3 + H_2SO_4 \rightarrow CaSO_4 \cdot 2H_2O \text{ (gypsum)} \quad (1)$$

$$CaCO_3 \rightarrow CaO + CO_2 \quad (2)$$

$$CaO + H_2SO_4 \rightarrow CaSO_4 \cdot 2H_2O \text{ (gypsum)} \quad (3)$$

$$CaO + H_2O \rightarrow Ca(OH)_2 \quad (4)$$

$$Ca(OH)_2 + H_2SO_4 \rightarrow CaSO_4 \cdot 2H_2O \text{ (gypsum)} \quad (5)$$

X-Ray diffraction. X-Ray diffraction measurement was accomplished using a Rigaku SE instrument and the XRD pattern was recorded in the 2θ range of 5–70 degrees. A ceramic copper tube (CuKα, λ = 1.54060 Å) was used as a source of X-rays, maintaining an external circulating cooling water system in the temperature range of 20–22 °C. The instrument maintained the current and voltage at 50 mA, and 40 kV, respectively. The Bragg–Brentano parafocusing geometry was maintained to collect data and maintain 0.01° steps both in the machine calibration and sample analysis. The accuracy of the instrument was confirmed by calibrating with the standard silicon reference and the pattern generated from the sample measurement was matched with the standard reference of the ICDD database (card no: #00-033-0311) provided in PDF 4. In addition to the phase analysis, the crystallographic properties were also estimated for better understanding of the characteristics of the synthesized materials. A series of parameters such as crystallite size, lattice parameters, microstrain, dislocation density, and crystallinity index were computed by eqn (6)–(10).[21,22]

$$\text{Crystallite size, } D_c = \frac{K\lambda}{\beta \cos\theta} \quad (6)$$

$$\text{Lattice parameters,} \frac{1}{d^2} = \frac{1}{\sin^2\beta}\left(\frac{h^2}{a^2} + \frac{k^2\sin^2\beta}{b^2} + \frac{l^2}{c^2}\right) - \frac{2hl\cos\beta}{ac} \quad (7)$$

$$\text{Crystallinity index, CI} = \frac{H_{(020)} + H_{(041)} + H_{(-151)}}{H_{(021)}} \quad (8)$$

$$\text{Dislocation density, } \delta = \frac{1}{(D_c)^2} \quad (9)$$

$$\text{Microstrain, } \varepsilon = \frac{\beta}{4\tan\theta} \quad (10)$$

In the above equations, Scherrer's constant $K = 0.94$; β = FWHM (full width at half maximum) (in radians); λ = wavelength of the X-ray source; θ = diffraction angle; a, b, c and h, k, l = crystallographic lattice parameters; $H_{(hkl)}$ = peak height of the (hkl) plane.

FT-IR spectroscopic analysis. An IR-Prestige 21 (Shimadzu, Japan) instrument was used to record the IR spectrum of synthesized gypsum, and an attenuated total reflection (ATR) accessory was embedded within the system. The data were collected by maintaining the transmittance mode in the range of 400 to 4000 cm^{-1} and maintaining a spectral resolution of 4 cm^{-1}. The visualized data were the average of 30 scans.

Scanning electron microscopy analysis. Morphological images were captured using a Phenom Pro scanning electron microscopy (SEM) instrument. The samples were in two forms: (i) in suspension form with pure ethanol; and (ii) direct solid powder form. A simple hair dryer was used to dry the samples. Images were captured by applying a 10 kV accelerating voltage.

Preparation of soil extract. Around 2 kg of surface soil was collected from different parts of a field close to the IGCRT laboratory and then mixed thoroughly after grinding. 250 g soil was mixed with 2 L DI water and stirred for 24 h employing a magnetic stirrer. Then, the solution was filtered using vacuum filtration apparatus, and 20 fold dilution was applied to the liquid part to accomplish the next procedures. The prepared soil extract was kept in an air tight sample bottle until further use.

Determination of free water. 50 g finely ground synthesized gypsum sample was first heated in a laboratory oven at 45 ± 2 °C temperature for 4 h and then subsequently cooled in an air-tight sample bottle. After reaching room temperature (25 °C), the sample was carefully weighed again. From the difference of these two weights, the mass percentage of free water was calculated using eqn (11) and the procedure was based on the Indian standard.[23]

$$\text{Free water (mass percentage)}_{45°C} = \frac{\text{Weight}_{initial} - \text{Weight}_{final}}{\text{Weight}_{initial}} \times 100 \quad (11)$$

Calculation of combined water. To estimate the combined water mass percentage accurately, 5 g of gypsum was measured and placed in a ceramic crucible. Then, the sample was heated at 210 ± 5 °C for 4 h and cooled down to room temperature in a glass sample bottle. From the variation of weight, the combined water percentage was computed using eqn (12) based on the

Indian standard.[23]

$$\text{Combined water (mass percentage)}_{210°C}$$
$$= \frac{\text{Weight}_{initial} - \text{Weight}_{final}}{\text{Weight}_{initial}} \times 100 \quad (12)$$

Behavior in water and soil extract. To examine the nature of synthesized gypsum in DI water and soil extract (as previously described in detail) a solution was prepared using a 1:80 ratio in both cases. Before measuring the different parameters, the multimeter was calibrated using a set of buffer solutions. A number of parameters such as pH, electrical conductivity, total dissolved solid (TDS), salinity, and potential difference were measured. The details of this procedure are documented elsewhere with variation of the solid to liquid ratio.[24–27]

Results and discussion

Thermogravimetric analysis

The thermal behavior of the synthesized gypsum was evaluated by performing thermogravimetric (TG) and differential scanning calorimetric (DSC) analyses as shown in Fig. 1. The gypsum contained two moles of water in its crystal structure which started to be released after 100 °C temperature and the release was sustained up to 200 °C. This dehydration process may be a combination of several steps but they combined with each other to generate a single strong peak which is confirmed by the DTG curve in Fig. 2. The dehydration of the gypsum was well defined by the endothermic peak which was initiated at 100 °C and continued up to 200 °C temperature. Up to 400 °C, no significant peaks were observed in the TG and DSC curves, but after this temperature the mass slowly started to change. A similar result for the thermal nature of gypsum was reported previously.[28] In the DSC plot, one exothermic peak originated at 950 °C temperature which may result from the crystallization of the calcium sulphate phase. No significant mass loss was observed near 950 °C which was also clearly observed in the DTG curve which presented no strong peaks. The total mass loss of the gypsum was nearly 77% up to 900 °C temperature
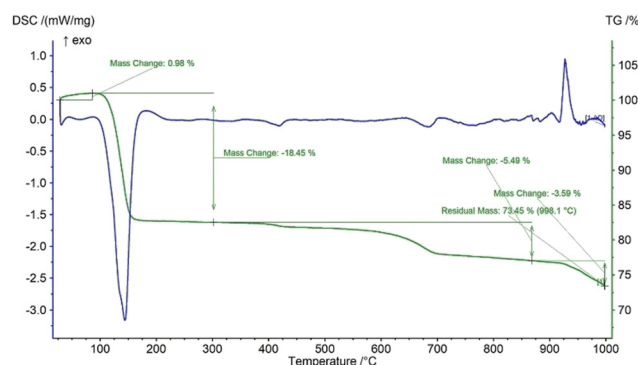

Fig. 1 Thermogravimetric (TG) and differential scanning calorimetric (DSC) analyses of gypsum synthesized from eggshells.
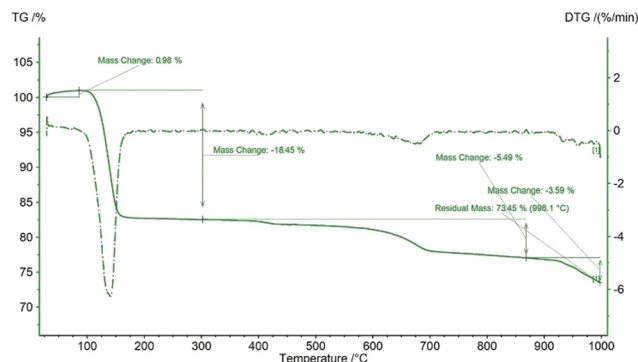
Fig. 2 TG and DTG curves of the synthesized gypsum.

which was very close to the theoretical mass loss due to the removal of two moles of water.

X-Ray diffraction analysis

The crystallographic parameters and phase of the synthesized product were explored by employing the X-ray powder diffraction method and the corresponding pattern is presented in Fig. 3. All the significant peaks registered for the mentioned standard were also observed for the synthesized products, and the notable 2θ values and planes are 11.64° (020), 20.75° (021), 23.39° (040), 29.17° (041), 31.11° (−221), 33.38° (220), 34.51° (−151), 35.96° (−202), 36.63° (022), 40.66° (151), 45.51° (−171), 47.83° (080), 50.32° (062), 51.50° (−262), 56.74° (190), 63.70° (−372), and 68.67° (262). From the similarity of the XRD data it was assumed that the synthesized product was gypsum ($CaSO_4 \cdot 2H_2O$). No undefined/unmatched peaks corresponding to secondary products were noticed in the XRD pattern. Thus, the gypsum was produced as a single phase compound.

The crystallite size was calculated by employing Scherrer's equation (eqn (6)) and the obtained value was 123 nm. The lattice parameters were estimated from eqn (9) and the measured values were $a = 6.24$, $b = 15.18$, and $c = 5.65$ Å which were very close to the standard database (card no: #00-033-0311) values
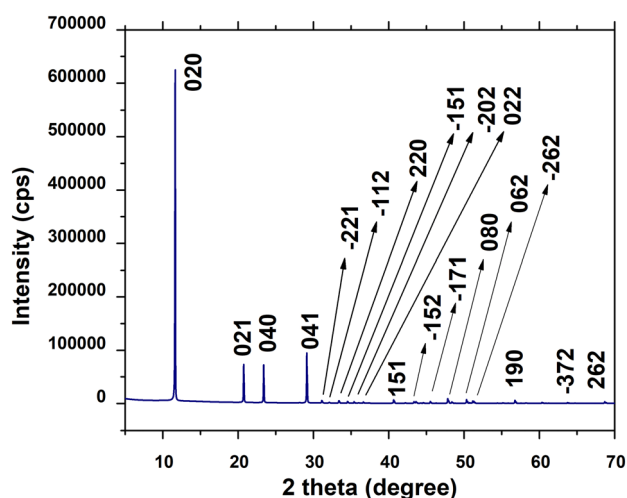

Fig. 3 XRD analysis of gypsum.

for the gypsum monoclinic crystal structure with the space group $C2/c$ (15). The dislocation density and microstrain were computed with the aid of eqn (9) and (10) and the generated values are 0.0654 lines m^{-2} and 0.1583%, respectively.

The relative intensity is also an important parameter and can be measured from the XRD data. Hence, for the (020) plane the relative intensity was estimated from the other three strong reflections for the (021), (040), and (041) planes. The relative intensity of the (020) plane can be represented as shown in eqn (13):[29]

$$\mathrm{RI} = \frac{I_{(020)}}{I_{(021)} + I_{(040)} + I_{(041)}} \qquad (13)$$

In the equation, the plane is shown in subscript. Following eqn (13), the relative intensity of the standard (card no: #00-033-0311) was also calculated for the same plane. The relative intensities of the measured sample and the standard were 2.144, and 0.52, respectively.

The preferential growth of the (020) plane was determined from eqn (14):[30]

$$\text{Preferential growth}, P = \frac{\mathrm{RI}(\text{sample}) - \mathrm{RI_s}(\text{standard})}{\mathrm{RI_s}(\text{standard})} \qquad (14)$$

The calculated preferential growth (P) for the gypsum sample at the (020) plane was 3.123. The positive value of the preference indicated that the growth along the (020) plane is stable and favorable which led to the formation of stable crystals. By employing the same procedure, the growth preference of all the planes can be measured and sometimes negative values can be found which indicate less stable planes.

Rietveld refinement

Rietveld refinement was performed to quantify and explain the percentage of gypsum phase in the synthesized product. Although the produced reflections from the powder XRD were easily separable, the Rietveld refinement was performed where 1.7% calcium sulphate phase was found along with 98.3% gypsum phase. In addition to this quantification the lattice parameters, namely a, b, and c were also refined. The refined lattice parameters of the gypsum phase were $a = 6.28$, $b = 15.199$, and $c = 5.67$ Å, which were very close to the measured parameters mentioned in the previous section. After Rietveld refinement the lattice parameters were exactly matched with the standard card no: #00-033-0311.

FT-IR spectroscopic analysis

Functional groups were identified utilizing Fourier Transform Infrared Spectroscopy (FT-IR) in the range of 4000–500 cm^{-1} and the spectrum is shown in Fig. 4. The functional groups associated with the produced compound are the sulphate and hydroxyl groups which are characterized by the bending, symmetric stretching, and asymmetric stretching vibrations in the mid-infrared region. In the region of 600 and 660 cm^{-1}, two peaks were noticed due to the bending vibration of the SO_4^{2-} group. Similar types of bending vibrations were reported
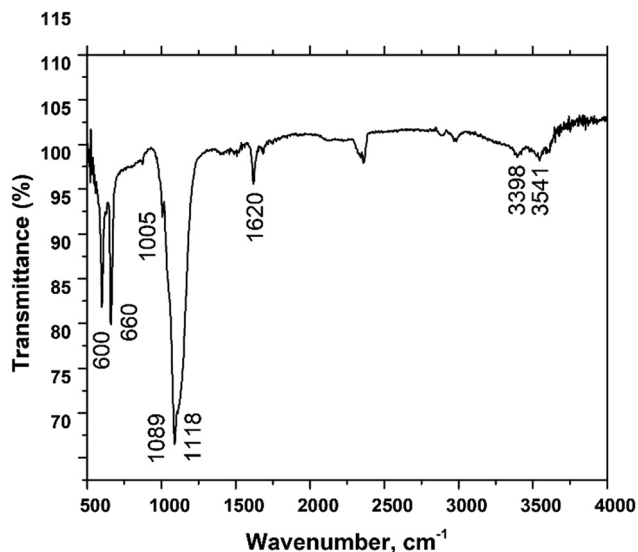
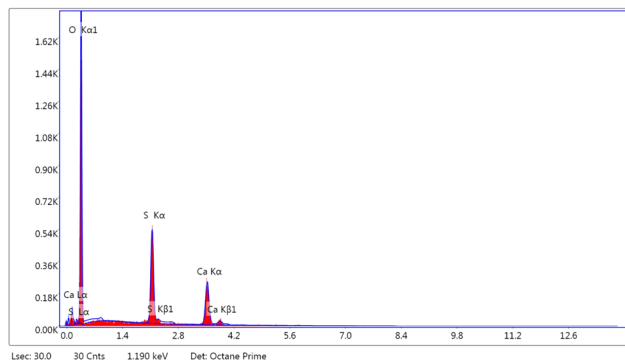**Fig. 4** Functional group analysis of gypsum.

Fig. 6 EDX spectrum of the synthesized gypsum.

group. The symmetric and asymmetric stretching vibration modes resulted in peaks in the regions of 3398 and 3541 cm^{-1}. These stretching vibration bands originated from the presence of water, which is supported by the literature.[33]

Surface morphology analysis

Surface morphological analysis was performed using SEM and the images captured at different magnifications are presented in Fig. 5. Variations in particle shape are noticed in the images of gypsum samples. The particles remained in clusters, forming
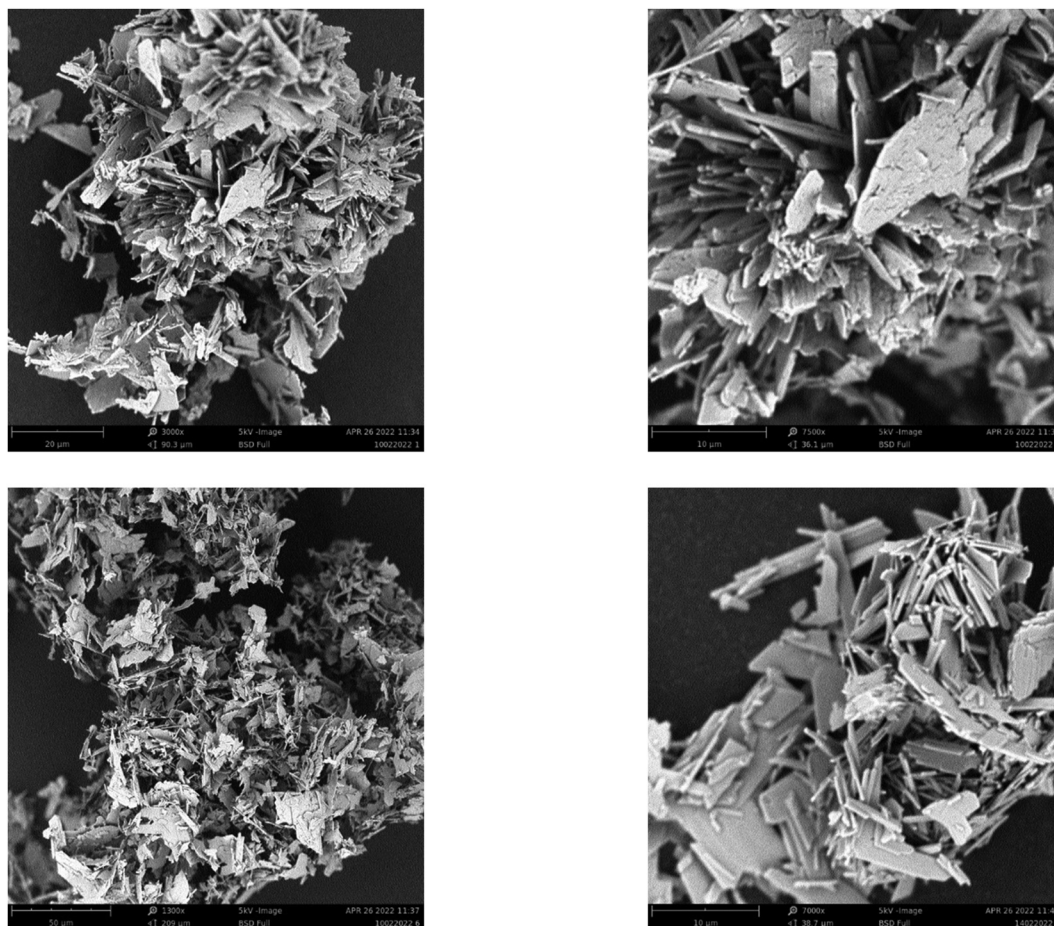
in the literature.[31,32] On the other hand, an asymmetric stretching vibration was observed in the region of 1118 cm^{-1} due to the presence of the SO_4^{2-} group. The peaks at 1622 and 1687 cm^{-1} originated from the bending vibration of the H–O–H

Fig. 5 SEM images of synthesized gypsum fertilizer.

Table 1 Change in pH, EC, TDS, salinity, and PD in aqueous media and soil extract for the gypsum

	Water	DI + gypsum			DI + soil	DI + soil + gypsum		
Parameter	DI	0 min	5 min	300 min		0 min	5 min	300 min
pH	7.19	10.29	10.67	10.63	8.63	10.11	10.44	10.64
EC (μS)	2.5	1519	1841	2214	33.5	1420	1520	1626
TDS (ppm)	19	921	1105	1324	20.4	836	866	975
Salinity (ppt)	35	1549	1842	2210	38.0	1409	1470	1527
PD (mV)	−11.5	−196	−217	−218	−89.6	−185	−190	−213

rod and plate shaped aggregates. As the reaction conditions were similar for different batches in gypsum synthesis, no significant variation was observed in the SEM images which were in tune with the FT-IR spectral analysis and XRD pattern matching. Although the gypsum was synthesized from naturally originating waste eggshells which are well known for identical particle sizes under SEM, there were significant variations in the particles within the gypsum. The images showed that the particles are broken into small particles from large shapes, and thus they showed affinity among the particles. Though there were variations in the compounds used as the raw source materials, dissimilarity among the particles of gypsum has been reported in a number of works.[34–36]

EDX analysis

The EDX spectrum recorded for the synthesized gypsum is shown in Fig. 6. The EDX data were good evidence for the presence of gypsum containing 26.17% calcium, 19.86% sulfur, and 53.97% oxygen and these values were very close to the theoretical values for gypsum, namely Ca-23.25%, S-18.6% and O-55.8%. A small variation was also noticed in the case of TGA data. This variation may be due to the presence of the calcium sulphate phase (1.7%) in gypsum which was quantified from the Rietveld refinement using XRD data.

Water percentage

The amount of water present in any sample as well as in fertilizer is very crucial for appropriate handling, storage, and application. In the case of the synthesized gypsum, free water and combined water (mass percentage) were computed as described in the methodology section. A very small amount of free water ($0.08 \pm 0.001\%$) was found in the gypsum sample. On the contrary, a higher percentage ($11.64 \pm 0.91\%$) of combined water was present in the sample and all the data was taken from the average of a minimum of 5 samples. Following the same procedure as described for combined water, at 150 °C the mass percentage of water was $7.38 \pm 0.54\%$. From the water percentage analysis, the moisture content of the final gypsum can be controlled without any difficulties.

Variation of behavior in aqueous media and soil extract

A significant variation was recorded in aqueous media and soil extract and the tests were performed as described in the previous section. A set of parameters such as pH, electrical conductivity (EC), total dissolved solid (TDS), salinity, and potential difference (PD) was measured and is recorded in Table 1. The pH of soil is very crucial for the appropriate growth of plants and the value is dependent on many factors. When gypsum was added to the water at a ratio of 1 : 80, the pH value changed significantly. Not only the pH value, but also the EC, TDS, salinity, and PD were also increased considerably. The same ratio of gypsum and soil extract gave very similar results. The experiment was carried out over 5 h, and a promising outcome was noted.

Conclusion

Gypsum fertilizer was synthesized successfully using three different routes and no distinct variation was noticed. Waste eggshells can be a potential source of calcium to produce valuable inorganic fertilizer which was supported by the results of XRD, FT-IR, and SEM. This research suggests that discarded parts of food can be utilized for a sustainable environment. There are sources of 80 million tons of eggshells, and small and medium industries can be established for the synthesis of gypsum fertilizer. When the synthesized gypsum was treated with aqueous medium and soil extract medium a significant change was noticed in the pH, conductivity, salinity and potential. As no authentic gypsum fertilizer synthesis procedure is freely available, this research can be a reference document.

Author contributions

Md. Sahadat Hossain conceived and designed the experiments, analysed the data, wrote the original manuscript, and performed the experiments. Md. Aftab Ali Shaikh carried out the TGA and EDX data analyses. Samina Ahmed supervised the overall work and assisted in writing the manuscript.

Conflicts of interest

There are no conflicts to declare.

Acknowledgements

References

1 Y. Dong and M. Z. Hauschild, Indicators for environmental sustainability, *Procedia CIRP*, 2017, **61**, 697–702.

2 J. C. Little, E. T. Hester and C. C. Carey, Assessing and enhancing environmental sustainability: a conceptual review, *Environ. Sci. Technol.*, 2016, **50**, 6830–6845.

3 M. Shafiee-Jood and X. Cai, Reducing food loss and waste to enhance food security and environmental sustainability, *Environ. Sci. Technol.*, 2016, **50**, 8432–8443.

4 Global Egg Production Continues to Grow, International Egg Commission, 2020, **https://www.internationalegg.com/resource/global-egg-production-continues-to-grow/** (accessed April 16, 2022).

5 M. Kristl, S. Jurak, M. Brus, V. Sem and J. Kristl, Evaluation of calcium carbonate in eggshells using thermal analysis, *J. Therm. Anal. Calorim.*, 2019, **138**, 2751–2758.

6 Ó. Ögmundarson, M. J. Herrgård, J. Forster, M. Z. Hauschild and P. Fantke, Addressing environmental sustainability of biochemicals, *Nature Sustainability*, 2020, **3**, 167–174.

7 T. A. Ahmed, L. Wu, M. Younes and M. Hincke, Biotechnological applications of eggshell: recent advances, *Front. Bioeng. Biotechnol.*, 2021, **9**, 548.

8 X. Meng and D. Deng, Trash to treasure: waste eggshells used as reactor and template for synthesis of Co_9S_8 nanorod arrays on carbon fibers for energy storage, *Chem. Mater.*, 2016, **28**, 3897–3904.

9 L. Li, T. Huang, S. He, X. Liu, Q. Chen, J. Chen and H. Cao, Waste eggshell membrane-templated synthesis of functional Cu^{2+}–Cu^{+}/biochar for an ultrasensitive electrochemical enzyme-free glucose sensor, *RSC Adv.*, 2021, **11**, 18994–18999.

10 M. Baláž, E. V. Boldyreva, D. Rybin, S. Pavlović, D. Rodríguez-Padrón, T. Mudrinić and R. Luque, State-of-the-art of eggshell waste in materials science: recent advances in catalysis, pharmaceutical applications, and mechanochemistry, *Front. Bioeng. Biotechnol.*, 2021, **8**, 612567.

11 L. Habte, N. Shiferaw, D. Mulatu, T. Thenepalli, R. Chilakala and J. W. Ahn, Synthesis of Nano-Calcium Oxide from Waste Eggshell by Sol–Gel Method, *Sustainability*, 2019, **11**, 3196, DOI: **10.3390/su11113196**.

12 S. Tanpure, V. Ghanwat, B. Shinde, K. Tanpure and S. Lawande, The Eggshell Waste Transformed Green and Efficient Synthesis of K-Ca(OH)$_2$ Catalyst for Room Temperature Synthesis of Chalcones, *Polycyclic Aromat. Compd.*, 2022, **42**, 1322–1340.

13 S.-C. Wu, H.-K. Tsou, H.-C. Hsu, S.-K. Hsu, S.-P. Liou and W.-F. Ho, A hydrothermal synthesis of eggshell and fruit waste extract to produce nanosized hydroxyapatite, *Ceram. Int.*, 2013, **39**, 8183–8188.

14 T. S. Kumar, K. Madhumathi and R. Jayasree, Eggshell waste: a gold mine for sustainable bioceramics, *J. Indian Inst. Sci.*, 2022, 1–22.

15 N. Laohavisuti, B. Boonchom, W. Boonmee, K. Chaiseeda and S. Seesanong, Simple recycling of biowaste eggshells to various calcium phosphates for specific industries, *Sci. Rep.*, 2021, **11**, 1–11.

16 K. Keshavarz, The effect of calcium sulfate (gypsum) in combination with different sources and forms of calcium carbonate on acid–base balance and eggshell quality, *Poult. Sci.*, 1991, **70**, 1723–1731.

17 J. Lim, C. A. Fernández, S. W. Lee and M. C. Hatzell, Ammonia and nitric acid demands for fertilizer use in 2050, *ACS Energy Lett.*, 2021, **6**, 3676–3685.

18 Gypsum, (n.d.). **https://www.natureswayresources.com/infosheets/gypsum.html** (accessed May 20, 2022).

19 T. D. Ginn and D. L. Gray, *Synthetic gypsum fertilizer product and method of making*, WO2014026048A2, 2014, **https://patents.google.com/patent/WO2014026048A2/en**, accessed May 20, 2022.

20 N. Tangboriboon, W. Unjan, W. Sangwan and A. Sirivat, Preparation of anhydrite from eggshell *via* pyrolysis, *Green Process. Synth.*, 2018, **7**, 139–146.

21 S. G. Dasari, P. Nagaraju, V. Yelsani, S. Tirumala and M. V. Ramana Reddy, Nanostructured indium oxide thin films as a room temperature toluene sensor, *ACS Omega*, 2021, **6**, 17442–17454.

22 S. Pal, R. Nisi, M. Stoppa and A. Licciulli, Silver-functionalized bacterial cellulose as antibacterial membrane for wound-healing applications, *ACS Omega*, 2017, **2**, 3632–3639.

23 Indian Standard: 1988-1982, IS 1288 (1982): Methods of test for mineral gypsum, Bureau of Indian Standard. 2 (n.d.) 1–20.

24 R. K. Schofield and A. W. Taylor, The measurement of soil pH, *Soil Sci. Soc. Am. J.*, 1955, **19**, 164–167.

25 R. O. Miller and D. E. Kissel, Comparison of soil pH methods on soils of North America, *Soil Sci. Soc. Am. J.*, 2010, **74**, 310–316.

26 N. James, Soil extract in soil microbiology, *Can. J. Microbiol.*, 1958, **4**, 363–370.

27 C. M. Nobile, M. N. Bravin, T. Becquer and J.-M. Paillat, Phosphorus sorption and availability in an andosol after a decade of organic or mineral fertilizer applications: Importance of pH and organic carbon modifications in soil as compared to phosphorus accumulation, *Chemosphere*, 2020, **239**, 124709.

28 K. Ghazi Wakili, E. Hugi, L. Wullschleger and T. H. Frank, Gypsum board in fire—modeling and experimental validation, *J. Fire Sci.*, 2007, **25**, 267–282.

29 H. Zanin, E. Saito, F. R. Marciano, H. J. Ceragioli, A. E. C. Granato, M. Porcionatto and A. O. Lobo, Fast preparation of nano-hydroxyapatite/superhydrophilic reduced graphene oxide composites for bioactive applications, *J. Mater. Chem. B*, 2013, **1**, 4947–4955.

30 M. Sharma, R. Nagar, V. K. Meena and S. Singh, Electrodeposition of bactericidal and corrosion-resistant hydroxyapatite nanoslabs, *RSC Adv.*, 2019, **9**, 11170–11178.

31 M. Al Dabbas, M. Y. Eisa and W. H. Kadhim, Estimation of gypsum-calcite percentages using a Fourier transform infrared spectrophotometer (FTIR), in Alexandria Gypsiferous Soil-Iraq, *Iraqi J. Sci.*, 2014, **55**, 1916–1926.

32 A. Kayabaş and E. Yildirim, New approaches with ATR-FTIR, SEM, and contact angle measurements in the adaptation to extreme conditions of some endemic *Gypsophila L.* taxa growing in gypsum habitats, *Spectrochim. Acta, Part A*, 2022, **270**, 120843.

33 B. Salvadori, V. Errico, M. Mauro, E. Melnik and L. Dei, Evaluation of gypsum and calcium oxalates in deteriorated mural paintings by quantitative FTIR spectroscopy, *Spectrosc. Lett.*, 2003, **36**, 501–513.

34 G. Camarini and S. M. Pinheiro, Microstructure of recycled gypsum plaster by SEM, *Advanced Materials Research*, Trans Tech Publications, 2014, pp. 243–246.

35 K. Kovler, Setting and Hardening of Gypsum-Portland Cement-Silica Fume Blends, Part 2: Early Strength, DTA, XRD, and SEM Observations, *Cem. Concr. Res.*, 1998, **28**, 523–531, DOI: 10.1016/S0008-8846(98)00004-0.

36 F. Matalkah, H. Bharadwaj, A. Balachandra and P. Soroushian, Development and characterization of gypsum-based binder, *Eur. J. Adv. Eng. Technol.*, 2017, **4**, 153–157.